24-088

Underground Mine Ramp Design for Beginners

William G. Pariseau
University of Utah, Salt Lake City, Utah

INTRODUCTION

Safety of mine ramps begins with an analysis of stress that almost certainly must be done numerically to take into account ramp geometry, route geology, rock properties, and pre-ramp stresses. The popular finite element method serves analysis purposes quite well. As a practical matter several obstacles to implementation need to be addressed including collection of rock and joint properties along the proposed ramp route, selection of ramp type, and specification of cross-section shape, size, and route grade. Additionally, stresses along the proposed route must be specified, preferably from in situ measurements.

One need not be an expert in numerical methods to proceed to ramp design, although a background in mechanics of materials and rock mechanics is essential, and a first course in numerical methods is quite helpful. The necessary software is easily brought to the design task, more accurately, to the task of design evaluation. This software also addresses other important mine design problems including design of safe (1) main entries in stratified ground, (2) barrier pillars, (3) bleeder entries, (4) inter-panel barrier pillars, (5) room and pillar mines, (6) shafts, and (7) "tunnels" (Pariseau 2022).

PROBLEM DEFINITION

The problem is to compute displacements and related strains induced by ramp excavation and the stresses that result, given ramp geometry, geology including rock properties, and pre-ramp stress. The combination of pre-ramp stress and stress change induced by ramp excavation allows for computation of elastic and yielding zone extents about the ramp section and beyond. This information provides useful guidance to safe ramp design in the form of element safety factor distributions.

A local element safety factor concept defined as the ratio of strength to stress requires definitions of suitable measures of strengths and stress for analysis. Both arise in the context of stress-strain relations. Strength may be defined as stress at the elastic limit, so in case of the famous Mohr-Coulomb criterion one has $fs = \tau_m(\text{strength})/\tau_m(\text{stress})$ which reduces to $fs = C_o/\sigma_c$ in unconfined compression and to $fs = T_o/\sigma_t$ in uniaxial tension where C_o and T_o are unconfined compressive and tensile strengths, respectively. Here τ_m is the maximum shear stress at failure. Alternatively, $fs = J_2^{N/2}$ (strength)/τ_m (stress) where J_2 is the second invariant of deviatoric stress (a measure of shear strength) and N is an exponent determined by testing, usually between one and two. This alternative also reduces to the unconfined compression and tension cases and has the advantage of including the effect of the intermediate principal stress on strength. When the formation is isotropic and N=1, this definition reduces to the well-known Drucker-Prager criterion.

PROBLEM APPROACH

Approach to the problem is by the finite element method and is easy as one-two-three. Step one requires specification of rock properties in the region of interest including elastic moduli and strengths. An elastic response to an initial application load followed by inelastic behavior is illustrated in Figure 1.

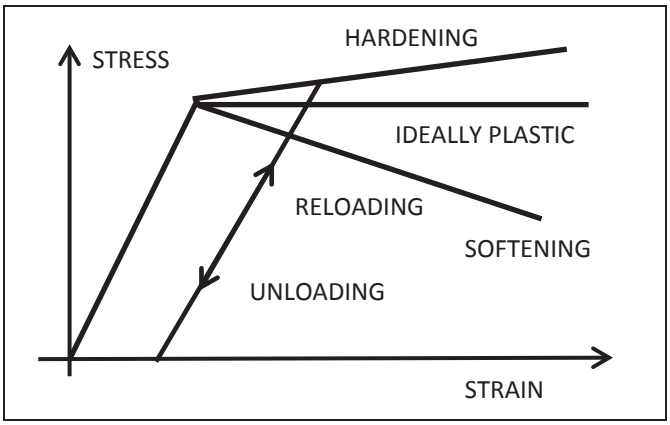

Figure 1. Idealized uniaxial stress-strain plots

Post-elastic behavior may be strain-hardening, softening or ideally elastic as seen in the figure (Pariseau 1999). Effects of joint sets on rock properties are readily included. Formation properties may be isotropic or anisotropic up to orthotropy with three axes of material symmetry.

Step 2 begins with a mesh that represents the geometry and geology of the considered ramp route. The mesh is a numerical model specified by computer files describing mostly element geometry but also boundary conditions and material behavior. Several common cross section shapes are available.

Mesh generation is easy and is done interactively with the aid of a computer program. First, the name of the rock properties file is requested, then the ramp type is called for (switchback or spiral). Grade is also requested and so it goes. All files needed for a finite element analysis are generated including a finite element run stream file. A short file that echoes input data is also generated. A visual mesh check is made possible by plotting the mesh using a convenient plotting program.

Step 3 is simply execution of the finite element run stream, perhaps after some simple editing. A tap on the executable finite element program file is all that is needed. Design evaluation follows from study of results, especially results in the form of element safety factor distributions.

EXAMPLE–SWITCHBACK (ZIG-ZAG) RAMP

This example relates to the former Homestake Mine in Lead, SD. This gold mine was developed to a depth of 8,000 ft (2,500 m) before closure and subsequent conversion to an underground research facility, the Sanford Underground Research Facility (SURF). Level interval at the mine is 150 ft (47.5 m). Ramps extended from surface to considerable depth.

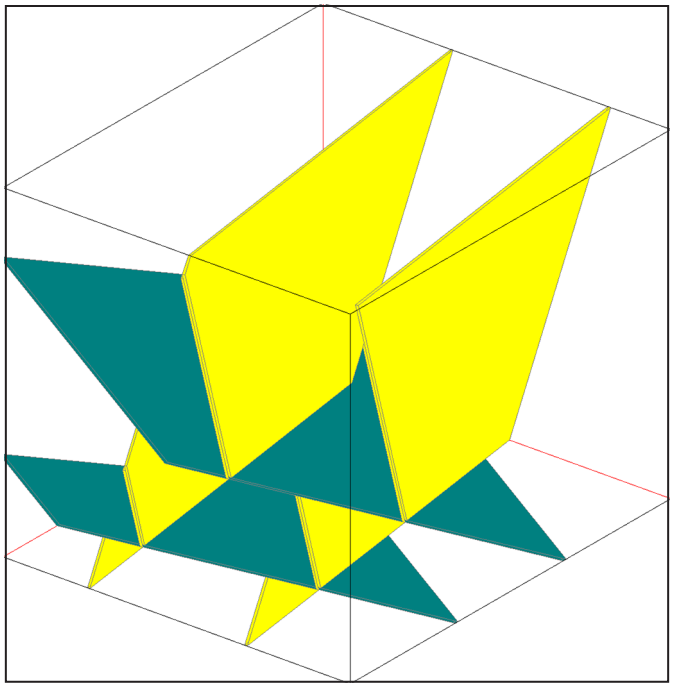

Figure 2. Schematic illustration of the two joint sets used in computing equivalent properties

Much rock mechanics data have been gathered through many studies during the operating life of the mine including stress measurements and formation properties (Pariseau 1985). The mine is located in Precambrian meta-sediments that impart distinct directional features to the rock. The Poorman formation formed the footwall; ore was located in the Homestake formation, and the Ellison formation formed the hanging wall. Laboratory testing of oriented drill core down the dip of the foliation, on strike and normal to the plane of the foliation suggested an orthotropic material model with three distinct directions *abc* of anisotropy (Duan 1985). The finite element axes are *xyz*. The axes of anisotropy are related to the reference axes by the dip direction and dip angles, α, δ. Depth to a particular formation and formation thickness are also specified in the material properties file.

*Step 1 Preparation of a materials property file S*pecification of formation properties includes effects of joint sets (Golder Associates 2010) illustrated in Figure 2.

The resulting equivalent rock properties are

```
NLYRS = 3
NSEAM = 3
 (1) Ellison
   0.288E+07  0.402E+07  0.389E+07    0.08   0.30   0.19
   0.218E+07  0.115E+07  0.890E+06    0.00   0.00   0.00
```

```
 5337.0    4926.3    7426.4    1105.6   999.3     386.6
 1402.5    1281.0     978.2
   90.0      70.0     3680.0     700.0
(2) Homestake
 0.272E+07  0.400E+07  0.391E+07   0.06   0.30    0.22
 0.191E+07  0.110E+07  0.913E+06   0.00   0.00    0.00
   9297.0    8847.9    7489.7    635.8   1280.2    738.8
   1403.7    1943.1    1358.1
    90.0      70.0     4380.0     120.0
(3) Poorman
 0.303E+07  0.407E+07  0.348E+07   0.09   0.31    0.18
 0.192E+07  0.117E+07  0.871E+06   0.00   0.00    0.00
   6459.5   6685.2    6947.7    1417.0    1040.6    569.7
   1746.7    1522.8    1148.6
    90.0      70.0     4500.0     700.0
```

The first two lines following the formation name are Young's moduli E and Poisson's ratios v; the second line contains shear moduli G and specific weight components γ (when gravity stresses are needed). The next two lines are unconfined compressive, tensile and shear strengths C, T and R. Units are psi. The last line gives the dip direction (deg), dip (deg), depth (ft) and thickness (ft) of the named formation. The equivalent strengths in this file are based on an energy-to-failure criterion. Full details are explained in a User Manual (Pariseau 2022).

Step 2 Mesh Generation Mesh generation input is saved in an InData file that is developed during mesh generation for the ramp. Thus,

```
Input Data
 "RAMPS" NPROB 9
 Ramps Shape = Arched Rectangle
 Ramp System = Single Opening
 Ramp Width =      11.0
 Width/Height Ratio =       1.0
 Ramp Height=      11.0
 Section Depth Seam Center (ft)   =    4850.0
 Additional Sxx,Syy=,Szz,Tyz,Tzx,Txy, tension +=psi
   -4648.0   -6062.0   -2788.0       0.0       0.0       0.0
 Ramp Stress Sxx,Syy=,Szz,Tyz,Tzx,Txy, tension +=psi
   -4648.0   -6062.0   -2788.0       0.0       0.0       0.0
```

No gravity stress is applied; rather, the premining stress is "additional" and based on formulas developed for the mine from many in situ stress measurements (Pariseau 1985). Stresses follow the section attitudes and are automatically rotated to the section orientation (dip and azimuth).

Boundary conditions are applied to the top, bottom and sides of the sections ("slabs") and prevent perpendicular displacement s ("rollers"). Normal displacements are also prevented on the external faces of the first and last sections.

A switchback ramp begins on the horizontal and then rapidly transitions to the design grade. The ramp transitions again to the horizontal at the ramp bottom. Figure 3 shows a mesh in longitudinal section of a ramp with a design grade of 15 percent. The mesh is mainly in the footwall Poorman formation in this simplified example. The uniform color (white) of the figure indicates the section is all in

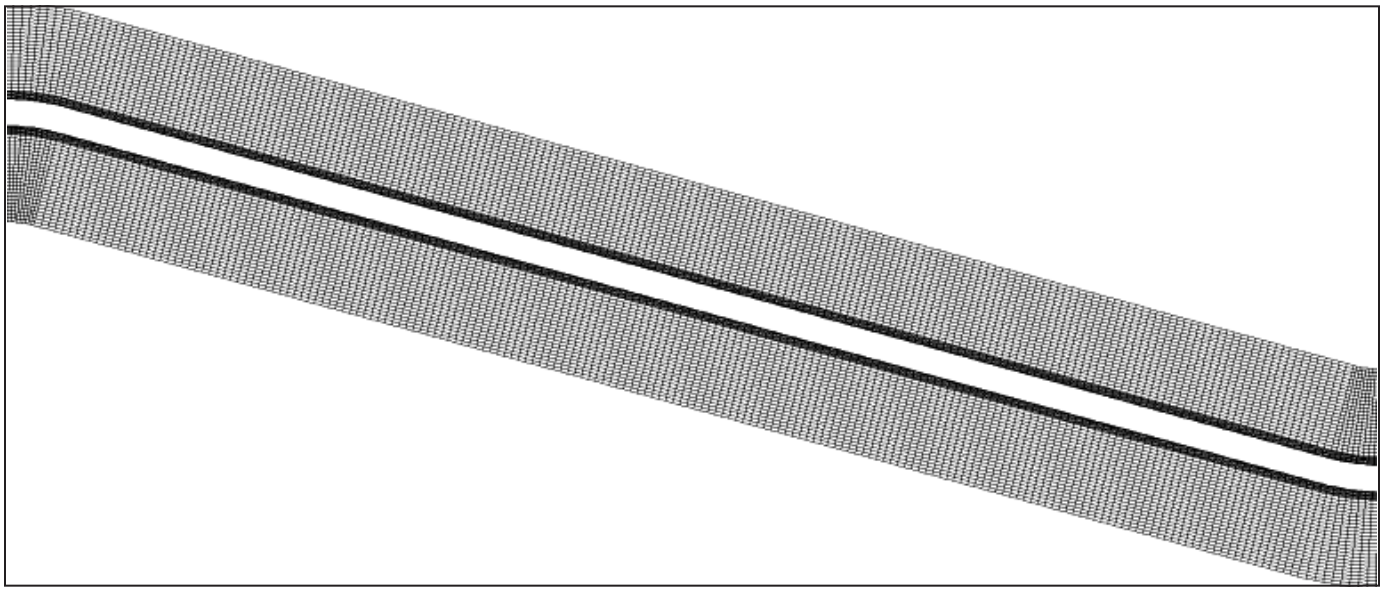

Figure 3. A long section of a switchback ramp with a design grade of 15 percent. The ramp is approximately 550 ft (168 m) long and declines 75 ft (23 m). Level interval is 150 ft (46 m)

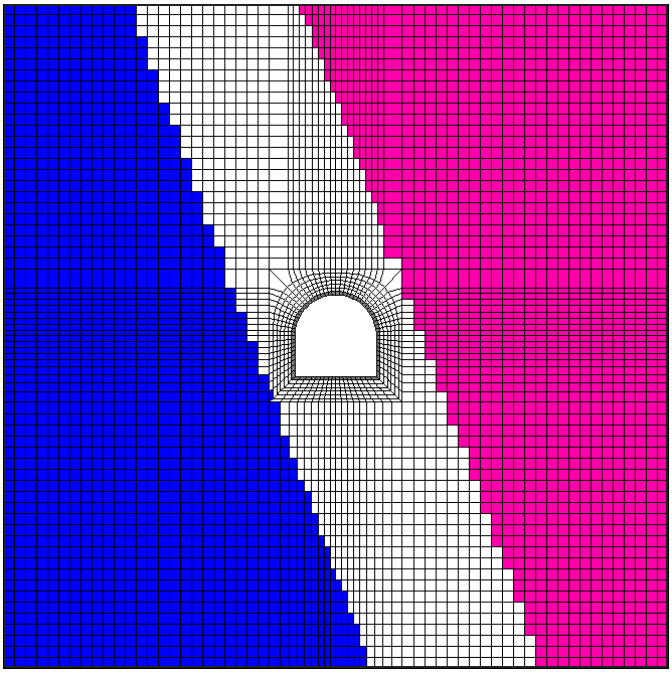

Figure 4. An arched back ramp cross-section in dipping rock formations indicated by the different colors. Grey elements indicate the boundary of the ramp section. The section is 11 ft (3.3 m) wide and has a width to height ratio of one

the same rock type (Poorman). Figure 4 shows the ramp in cross-section and the three major rock formations present.

Step 3 FEM Execution and Results The runstream file produced during mesh generation is

```
HME Drift energy to failure equiprops 4/23/2023 zigzag
Studio 2010\Projects\SPK\GMB3\EQHMEdrift.txt
F:\Visual Studio 2010\Projects\SPK\GMB3\belms
F:\Visual Studio 2010\Projects\SPK\GMB3\bcrds
F:\Visual Studio 2010\Projects\SPK\GMB3\brcte
F:\Visual Studio 2010\Projects\SPK\GMB3\bsigi
F:\Visual Studio 2010\Projects\SPK\GMB3\bnsps
HMRz
nelem =  907200
nnode =  945504
nspec =   53064
nmat  =       3
ncut  =      -1
ninc  =       5
nisgo =       1
inter =     200
maxit =    4000
nyeld =       2
nelcf =   14400
nsol  =       2
nprb  =       9
mgob  =       0
 error=    1.0000
 orf  =    1.8600
 xfac =   12.0000
 yfac =   12.0000
 zfac =   12.0000
 efac =    1.0000
 cfac =    1.0000
tolr% =    0.0100
ENDRUN
```

Figure 5 shows the distribution of element safety factors in a cross section at the top of the ramp and Figure 6 shows the element safety factor distribution in a long section. The distribution changes little with additional depth which is not too surprising since the change in depth going down the ramp is only an additional 75 ft. Depth of the section is approximately 4,850 ft. Some bolting and perhaps screening is indicated by the failures at corners and shoulders of the ramps

EXAMPLE–SPIRAL RAMP

This example is inspired by a ramp at the famous Lucky Friday Mine in the Coeur d'Alene Mining District of Northern Idaho (Williams et al 1992). As usual, the study process proceeds in three steps.

Step 1 Preparation of a materials property file The equivalent properties are (units are as before):

```
NLYRS = 3
NSEAM = 2
  (1) Vitreous Quartzite N50W 70SW
  0.272E+06   0.624E+05   0.350E+06     0.10   0.01     0.21
  0.479E+05   0.161E+06   0.342E+05     0.00   0.00     0.00
    5172.5    2477.4      5867.8       591.1      283.1      670.6
     1009.6      483.5     1145.3
      220.0       70.0     4720.0       280.0
  (2) Argillitic Quartzite modified for the HOOK at 5100
  0.258E+06   0.620E+05   0.298E+06   0.11   0.01     0.18
  0.473E+05   0.152E+06   0.340E+05   0.00   0.00     0.00
    2106.0    1032.4      4976.7     691.3      338.9      439.5
     696.6      341.5      853.9
      220.0       70.0     5100.0       40.0
  (3)  Sericitic Quartzite
  0.268E+06   0.623E+05   0.337E+06   0.10   0.01     0.20
  0.478E+05   0.159E+06   0.342E+05   0.00   0.00     0.00
    3858.9    1858.9      7557.9     514.7      247.9      444.1
     813.6      392.0     1057.7
      220.0       70.0     5240.0       280.0
```

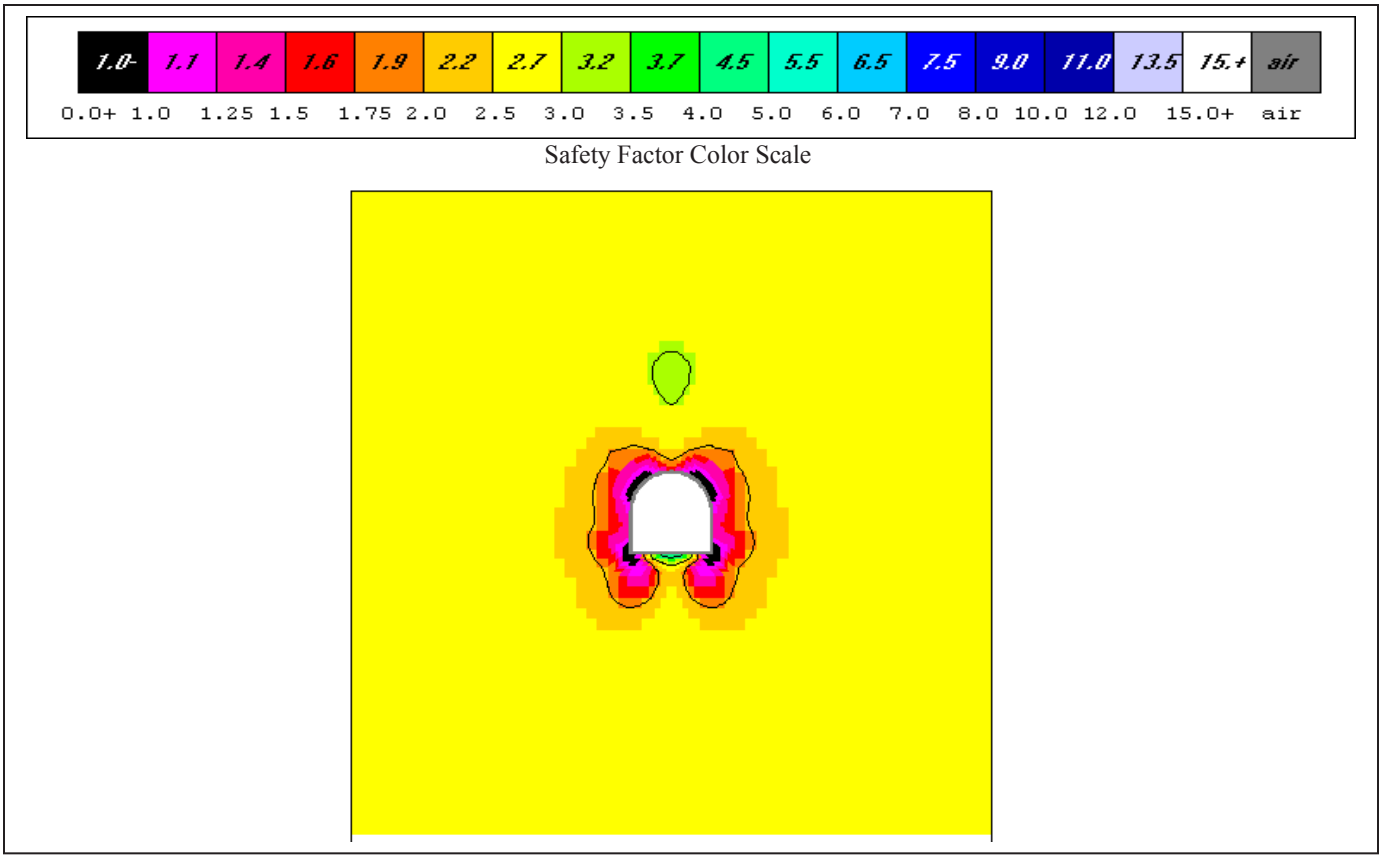

Figure 5. Element safety factor distribution in a cross section at the ramp top. The section is 11 ft (3.4 m) wide

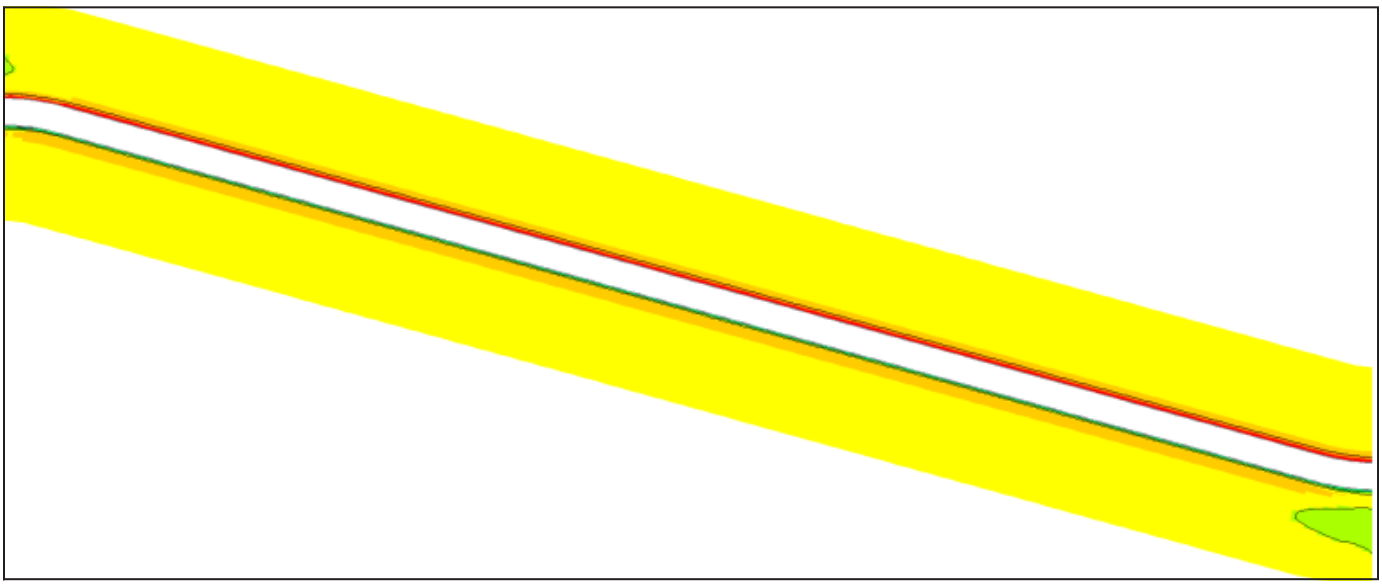

Figure 6. Element safety factor distribution in long section. Inclination of the section and the small increase in depth matter little in the safety factor distribution seen in cross-section

where depth is 5120 ft (1,5161 m). The ramp is in argillitic quartzite (NSEAM=2).

Elastic and strength properties are anisotropic as evident in the file. Interestingly, the original properties are also anisotropic. For example in case of argillitic quartzite,

```
(1) joint S70W 0.1 thik N=2
  4.2e+04   4.2e+04   1.8e+04      0.18      0.11      0.11
  1.1e+04   1.1e+04   1.8e+04       0.0       0.0       0.0
    850.0     850.0    1223.0     279.0     279.0     108.0
    282.0     282.0     210.0
    350.0      65.0       0.5     -0.10
 (2) joint  N=2
  4.2e+04   4.2e+04   1.8e+04      0.18      0.11      0.11
  1.1e+04   1.1e+04   1.8e+04       0.0       0.0       0.0
    850.0     850.0    1223.0     279.0     279.0     108.0
    282.0     282.0     210.0
    355.0      89.0       0.5     -0.10
 (3) joint bedding plane N=2
  4.2e+04   4.2e+04   1.8e+04      0.18      0.11      0.11
  1.1e+04   1.1e+04   1.8e+04       0.0       0.0       0.0
    850.0     850.0    1223.0     279.0     279.0     108.0
    282.0     282.0     210.0
    220.0      70.0       1.0     -0.10
  (2) Argillitic Quartzite
  4.2e+06   4.2e+06   1.8e+06      0.18      0.11      0.11
  1.1e+06   1.1e+06   1.8e+06       0.0       0.0       0.0
   8500.0    8500.0   12230.0    2790.0    2790.0    1080.0
   2820.0    2820.0    2100.0
    220.0      70.0    5980.0      40.0
```

where joint stiffnesses (moduli) are estimated as one percent of the intact moduli and joint strengths are estimated as ten percent of intact rock strength. Units are as before. The depth of the argillitic quartzite is not important to the calculation of equivalent jointed rock properties, only in the finite element analysis following. The negative thickness is a flag to the computer program indicating a joint.

Step 2 Mesh Generation Mesh generation input is given in the InData file that is developed during mesh generation for the drift section. Thus,

```
Input Data
 "RAMPS" NPROB 9
 Ramps Shape = Arched Rectangle
 Ramp System = Single Opening
 Ramp Width =      11.0
 Width/Height Ratio =       1.0
 Ramp Height=      11.0
 Section Depth Seam Center (ft)   =    5120.0
 Additional Sxx,Syy=,Szz,Tyz,Tzx,Txy, tension +=psi
   -7721.0   -5774.0   -5906.0       0.0       0.0       0.0
 Ramp Stress Sxx,Syy=,Szz,Tyz,Tzx,Txy, tension +=psi
   -7721.0   -5774.0   -5906.0       0.0       0.0       0.0
      0.0       0.0       0.0
```

No gravity stress is applied; rather, the premining stress is "additional" and based on formulas developed from many in situ stress measurements (Board and Beus 1989).

A spiral ramp begins on a level grade and then begins to decline according to the design grade in a circular path for 360 deg or more as desired. Figure 7 shows the mesh

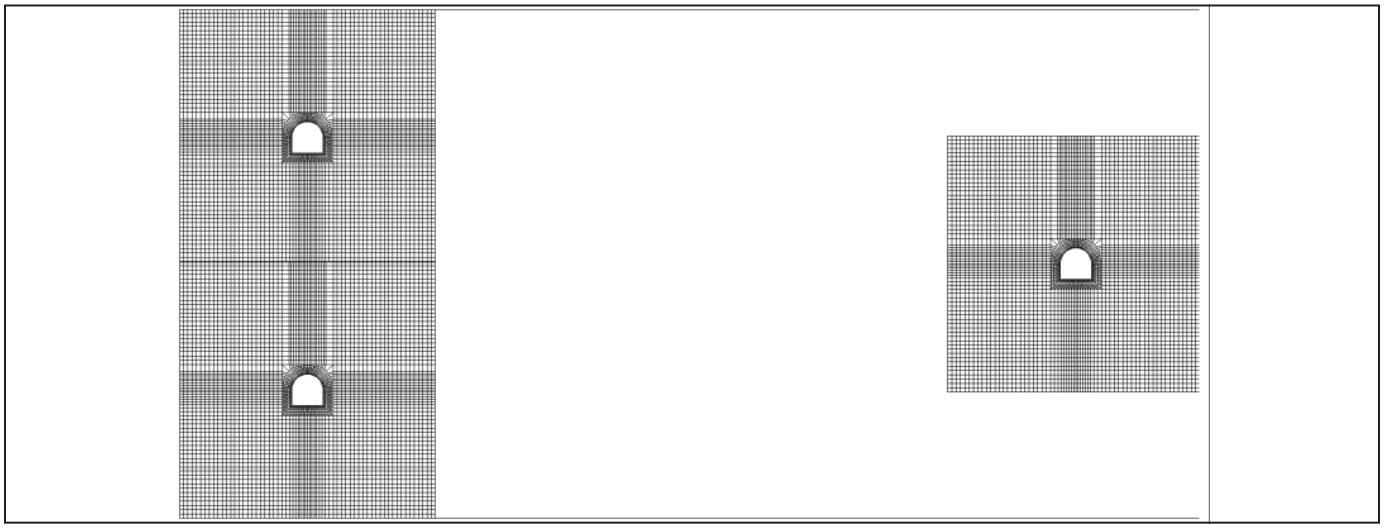

Figure 7. A cross-section of a spiral ramp with a design grade of 15 percent. The ramp is circular so sections are at 0, 180 and 360 deg are shown. The section is 11x11 ft (3.4x3.4 m). The spiral radius is 11.25 times opening width or 123.74 ft (37.7 m)

in cross-section at design grade of 15 percent. There are two hundred sections in the mesh. Each section contains 4,536 elements. A refined mesh near the ramp walls insures satisfactory quality of numerical results. A less refined mesh away from the ramp walls provides economy of computation. The sections are at 0, 180 and 360 degree azimuths.

Step 3 FEM Execution and Results The runstream file produced during mesh generation is similar to the runstream in the previous example. Thus,

```
Lucky Friday 5100 Hook equiprops 4/26/2023 spiral wgp
F:\Visual Studio 2010\Projects\SPK\GMB3\EQLFM.txt
F:\Visual Studio 2010\Projects\SPK\GMB3\belms
F:\Visual Studio 2010\Projects\SPK\GMB3\bcrds
F:\Visual Studio 2010\Projects\SPK\GMB3\brcte
F:\Visual Studio 2010\Projects\SPK\GMB3\bsigi
F:\Visual Studio 2010\Projects\SPK\GMB3\bnsps
LFMrS
nelem =  907200
nnode =  945504
nspec =  53064
nmat  =      3
ncut  =     -1
ninc  =      5
nisgo =      1
inter =    200
maxit =   4000
nyeld =      2
nelcf =  14400
nsol  =      2
nprb  =      9
mgob  =      0
 error=   1.0000
 orf  =   1.8600
 xfac =  12.0000
 yfac =  12.0000
 zfac =  12.0000
 efac =   1.0000
 cfac =   1.0000
tolr% =   0.0100
ENDRUN
```

This analysis required about six hours of runtime and resulted in 32,327 failed elements, about 3.6 percent of total elements.

Figure 8 shows the distribution of element safety factors in several cross sections of the ramp. The distributions change little with additional depth. Element failures (black)

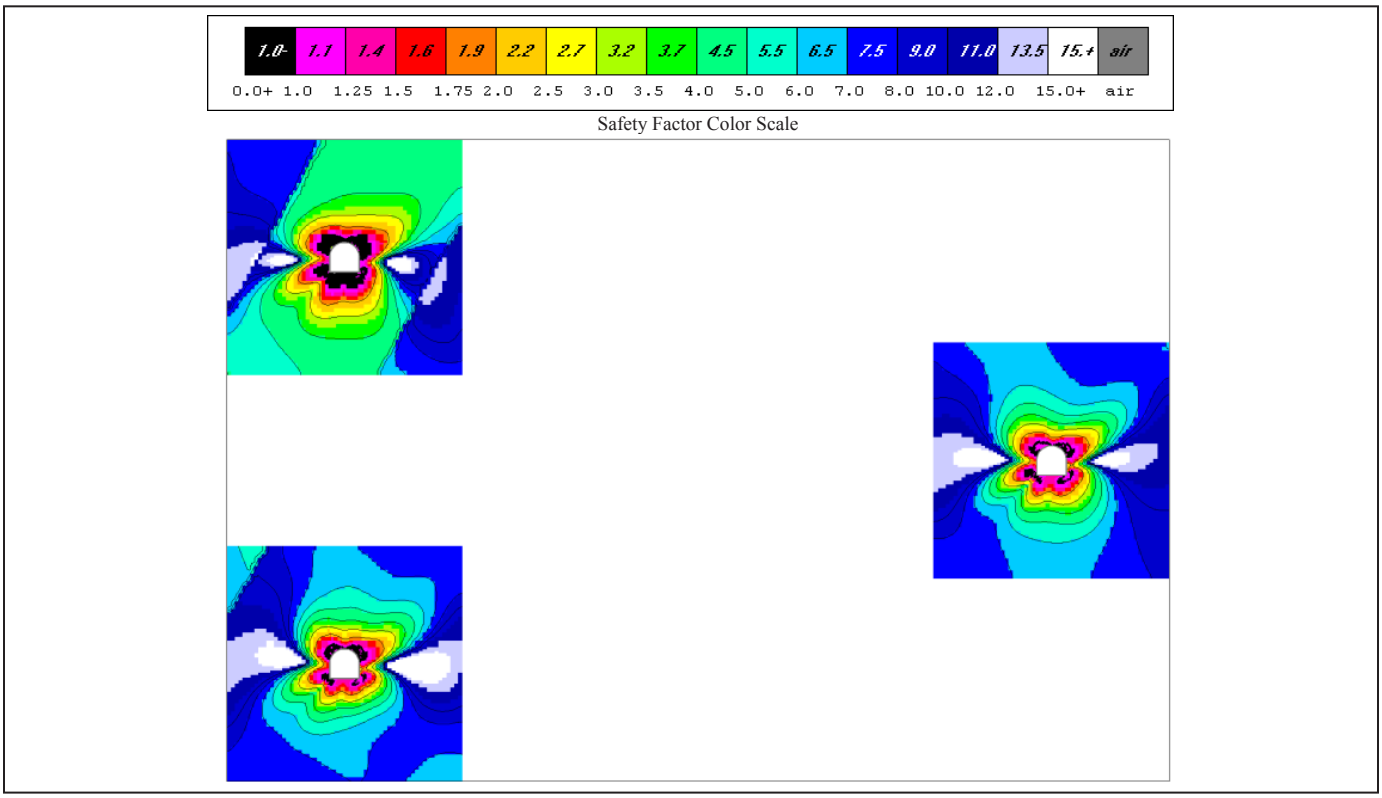

Figure 8. Element safety factor distributions in cross-sections of a 360 deg spiral ramp at the default ramp radius of 11.25 times opening width

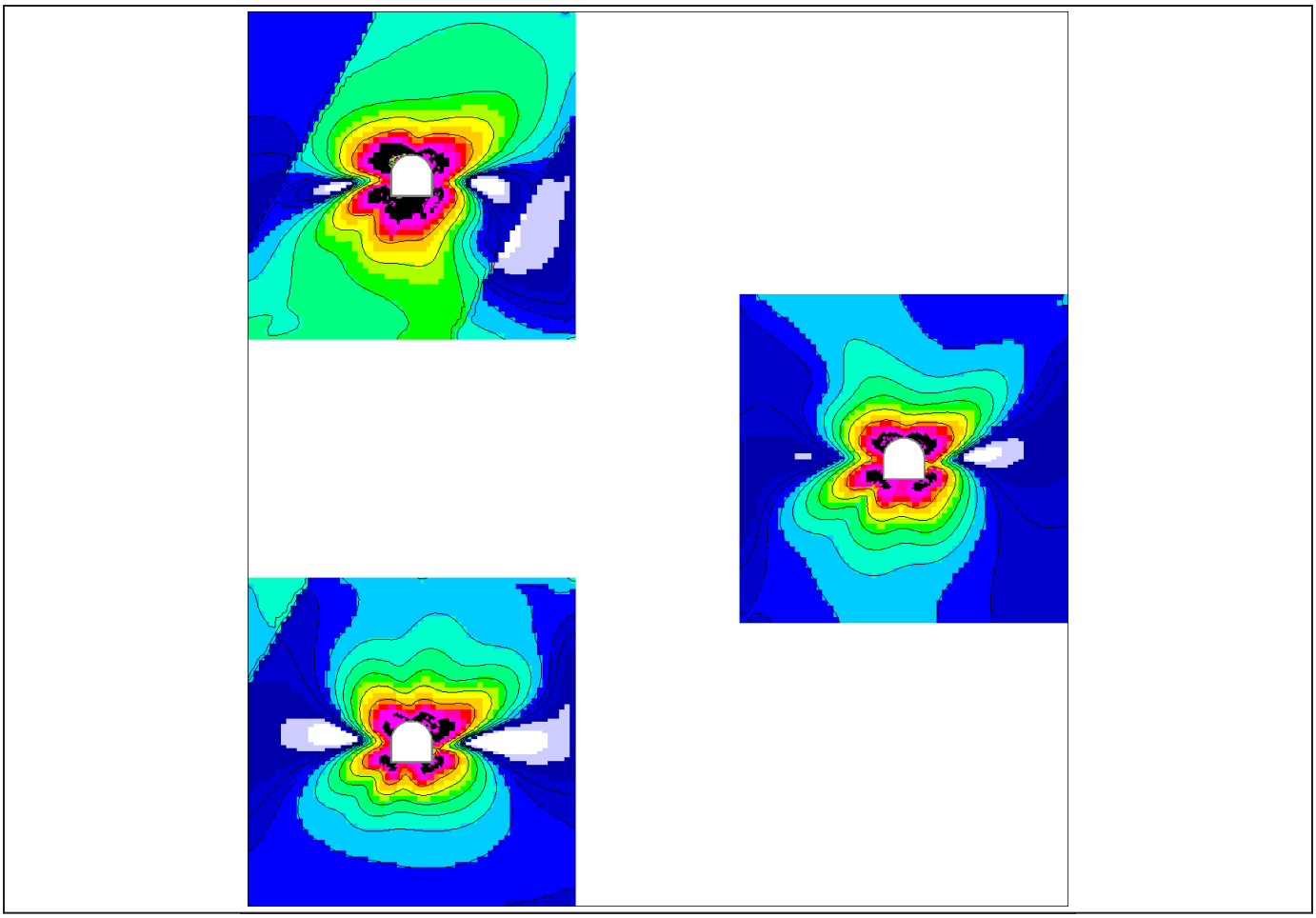

Figure 9. Element safety factor distributions in cross-sections of a 360 deg spiral ramp at one-half the default ramp radius

occur at the corners near the section bottoms and over the section shoulders where stress concentration is expected to be relatively high. Bolting and screening are indicated in this case. However, element safety factors increase rapidly with distance into the solid (indicated by color change from red to green and blue).

Ramp radius is set at a default value of 11.25 times opening width but can changed during mesh generation. There is no default ramp grade, but is also set during mesh generation.

Figure 9 shows the distribution of element safety factors in case of the ramp radius set at one-half the default value. In this case, approximately 4.8% of the elements have yielded. Thus, element failures are one-third more than the base case of the larger, defaults ramp radius case, although a visual comparison toes not indicate much difference.

Figure 10 shows the distribution of element safety factors in case of the ramp radius set at the minimum value of mesh width. In this case, approximately 5.2% of the elements have yielded. Thus, element failures are 44% more than the base case of the larger, defaults ramp radius case, although a visual comparison toes not indicate much difference. The number of 360 deg loops in the spiral can be varied also.

CONCLUSION

Mine ramps are important features of many underground mines but are not easy to design because of ramp geometry and geology. However, software specially formulated to accommodate ramp complexity makes design as easy as one-two-three. The first and most difficult step is the specification of rock formation and joint set properties in the region of interest. Elastic moduli, strengths, formation depths, thicknesses, and directions are needed and joint set properties, as well. The second step is mesh generation and is done interactively with specification of ramp section shape, ramp type (zig-zag, spiral), starting depth and grade. Mesh plotting is also easy once generated and allows for visual checking. A finite element runstream file is generated during this second step. The third step is execution

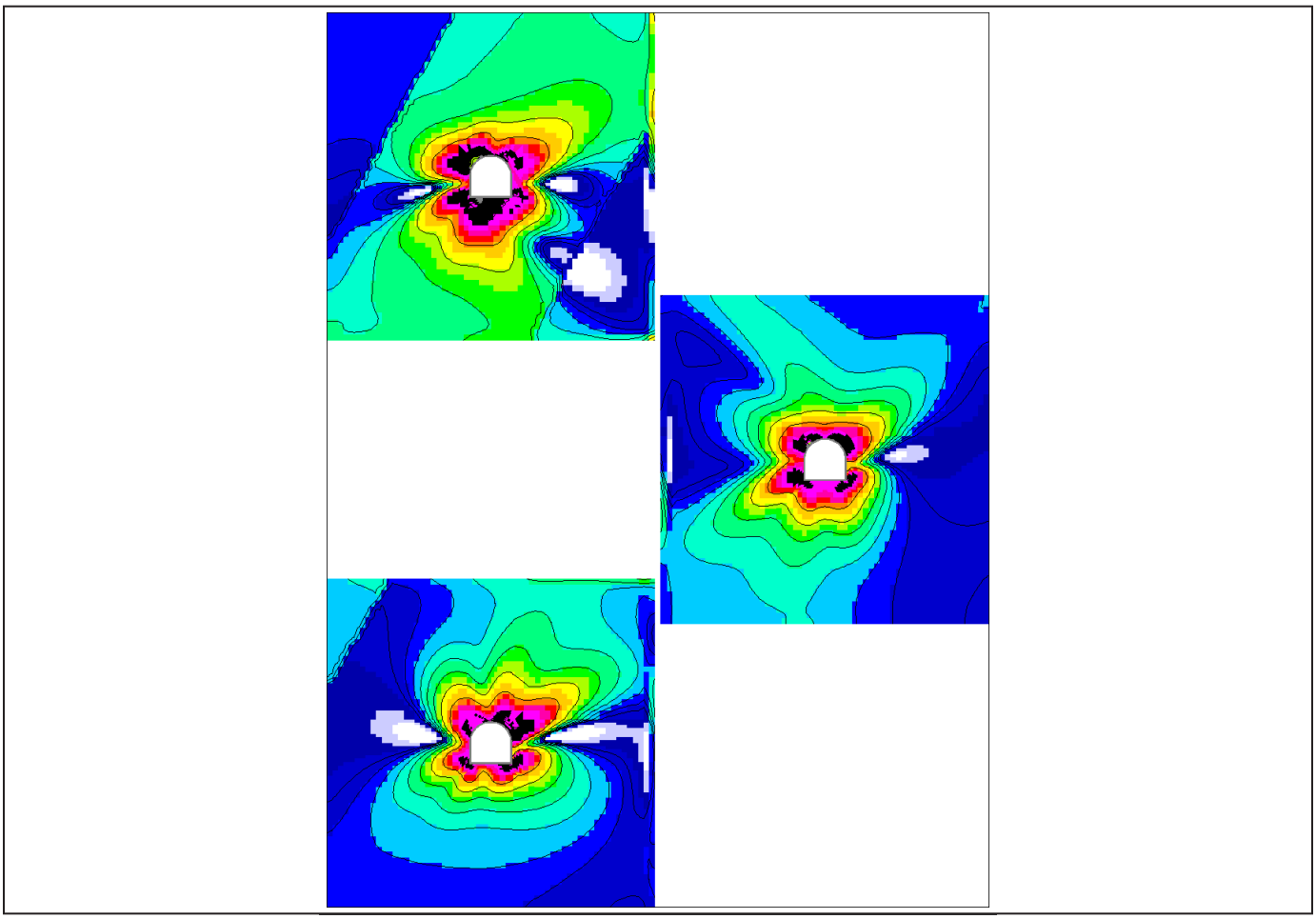

Figure 10. Element safety factor distributions in cross-sections of a 360 deg spiral ramp at the minimum ramp radius

of the ramp runstream file using the popular finite element method for computation of displacement and strain induced by excavation and resulting stress. Yielding occurs in elements that reach the elastic limit, so the extent of elastic and yielding zones are evident in an output file containing element safety factors. Plotting of element safety factors is easily done and provides design guidance. Should the results show extensive yielding, a new design is readily done by repeating the three step process with appropriate changes in ramp geometry and perhaps location. A user manual provides similar process details to several other important mine design problems (Pariseau 2022).

REFERENCES

Board, M. P. and M. J. Beus *In situ Measurements and Preliminary Desgin Analysis for Deep Mine Shafts in Highly Stressed Rock.* U.S.B.M. RI 9231.

Duan, F. (1985) Report on Rock Properties for the Homestake Mine. Internal Report, Department of Mining Engineering, University of Utah.

Golder Associates (2010) Preliminary Design Interim Report #3. Contract D10-04 Engineering and Design Services for Excavation—DUSEL.

Pariseau, W. G. (1985) "Research Study on Pillar Design for Vertical Crater Retreat (VCR)" U. S. Bureau of Mines Final Report, Contract J0215043 University of Utah.

Pariseau, W. G. (1999) "An Equivalent Plasticity Theory for Jointed Rock Masses." *Int'l J. Rock Mech. Mng. Sci.*, Vol. 36, No.7, pp. 907–918.

Pariseau, W. G. (2022) "User Manual for a Three-dimensional Finite Element Program UT3PC (2nd edition) A Fundamental Approach to Design of Coal Mine Entries, Barrier Pillars, Bleeder Entries, Interpanel Barrier Pillars, Pillars and Rooms in Room and Pillar Mines, Shafts and Tunnels." Website UT3PC.net.

Williams, T. J., J. K. Whyatt and M. E. Poad (1992) *Rock Mechanics Investigations a the Lucky Friday Mine (In Three Parts) 1. Instrumentation of an Experimental Underhand Longwall Stope*. U.S.B.M. RI 9432.

24-089

Unlocking Microbial Potential to Develop Innovative and Environmentally Responsible Technologies

Dan Stigers, Karrie Radloff, Michaeline Albright, Bianca Cruz, Tom Lankiewicz, Elizabeth Deyett, Dayal Saran, Kent Sorenson
Allonnia, Boston, MA

ABSTRACT

Biology opens a new frontier for the mining industry. With rising environmental concerns, the need to couple conventional chemical and physical technologies with sustainable approaches is pressing. At Allonnia, we harness microbial processes to create innovative and environmentally responsible technologies with broad applications. The native microbial community (microbiome) remains largely unexplored at most mining sites, unlike the geochemical environment. The exploration of complex biological reactions that could transform mining technology is just starting and holds vast possibilities, spanning bio-cementation, carbon sequestration, ore beneficiation, water mitigation, bioleaching, metals recovery, and more. Allonnia has collected samples from mine sites in Australia, Africa, and North America to characterize the microbiome and uncover the genetic potential present in mineral-rich environments. We are evaluating microbial metabolites that selectively solubilize gangue from various ores. In addition, biological reactions hold promise as tailings stabilizers. Our early efforts illustrate exciting prospects for harnessing biology's potential in mining.

INTRODUCTION

Our mission is to utilize known and novel biological processes to tackle some of the world's most pressing environmental challenges. We identified several processes essential to the mining industry that are naturally occurring at the microscale in microbial communities across the globe and have used this as both an inspiration and a starting point for transforming how these processes can be done at scale—to unlock untapped potential and to bring about more environmentally responsible technologies. To do this, we maintain and continue to build an industry-leading database of genetically sequenced and functionally characterized microbes and enzymes for biotransformation or biogeochemical sequestration of target compounds in various environments and media. We have identified two areas within the mining industry where known microbial processes play a key role: the solubilization of target elements and the controlled agglomeration of particles through the precipitation of carbonates.

The natural weathering of silicate and other materials by microbes present in the environment provides the starting point for the development of unique bio-solvents comprised of bacterial and/or fungal metabolites (Castro et al. 2000; Jain and Sharma, 2004; Torres et al., 2019, Li et al. 2019; Lamerand et al., 2020). The bio-solvents have several distinct advantages over conventional mineral acids such as sulfuric or hydrochloric acid (Dong et al. 2022). First, in addition to lowering the pH and promoting acidolysis, the bio-solvents provide ligands and chelators that form strong